A hands-on introduction to single photons and quantum mechanics for undergraduates

Brett J. Pearson[a] and David P. Jackson
Department of Physics and Astronomy, Dickinson College, Carlisle, Pennsylvania 17013

(Received 6 November 2009; accepted 10 February 2010)

We describe a series of experiments used in a sophomore-level quantum physics course that are designed to provide students with a hands-on introduction to quantum mechanics. By measuring correlations, we demonstrate that a helium-neon laser produces results consistent with a classical model of light. We then demonstrate that a light source derived from a spontaneous parametric down-conversion process produces results that can only be described using a quantum theory of light, thus providing a (nearly) single-photon source. These single photons are then sent into a Mach–Zehnder interferometer, and interference fringes are observed whenever the path of the photons cannot be determined. These experiments are investigated theoretically using straightforward quantum-mechanical calculations. © *2010 American Association of Physics Teachers.*
[DOI: 10.1119/1.3354986]

I. INTRODUCTION

This article describes our incorporation of single-photon experiments used in our second-year course titled "Introduction to Relativistic and Quantum Physics." Throughout the paper, we follow the experimental-based approach we use with our students, introducing concepts as needed to explain observed results. Most of the experiments described have been performed by others in both pedagogical and research settings. The goal of this paper is to offer a slightly different pedagogical approach than previously reported and to clarify some confusing aspects of these experiments. Because more departments will likely introduce similar experiments in the future, we hope others will find our approach useful. A secondary goal of this paper is to illustrate that the concept of a photon, on which most of these experiments rely, is more complex and subtle than students and physicists typically assume. Although we make no attempt to resolve this still-debated concept, we try to present our students, and therefore the reader, with enough information to clearly see the remaining complexities.

Because the experiments examine light, any attempt to glimpse into the quantum-mechanical world first requires a demonstration that light is quantized. In textbooks, the quantized nature of light is often introduced by discussing the photoelectric effect. However, although Einstein's explanation is beautifully simple, semiclassical theories, which treat light as a classical electromagnetic wave and only quantize the detector atoms, are capable of explaining the effect as well and did so as early as 1927.[1,2] Despite the success of Dirac's quantization of the electromagnetic field[3] and the development of quantum electrodynamics,[4] the semiclassical theory is sufficient to explain nearly all observations of light-matter interactions in the optical region of the spectrum.[5]

At first glance, it seems straightforward to demonstrate the existence of photons. Simply take a (very) dim light source, pass it through a beam splitter, and measure the transmission and reflection intensities with a sensitive detector. If light consists of quantized packets of energy, then we should never detect light at the two output ports simultaneously (in coincidence). As we will discuss in more detail, experiments are never perfect, and there is always a possibility of measuring an accidental coincidence by chance. The first detailed experiments examining such intensity correlations took place in 1956 when Hanbury Brown and Twiss measured second-order (intensity) correlations in light for applications in astronomical interferometry. By using an arclamp source, they observed more coincidences than would be expected by chance, in contrast to what would be naively expected from the photon model.[6,7] If the photon model is correct, these photons arrived in "bunches."

Although predicted by semiclassical theories, these results motivated a theoretical consideration of the statistical and coherence properties of light using a quantum-mechanical description.[8–10] This work, along with contributions from many others,[11–13] led to the foundation of modern quantum optics. Experiments examining the statistical properties of various light sources were performed by several groups,[14–17] culminating in the observation of photon "antibunching"—coincidence measurements less often than random—an effect that cannot be explained using a classical theory.[18] Although this effect requires a quantum-mechanical description of light, it was not until 1986 that experiments definitively showed that light hitting a beam splitter behaves as indivisible quanta or photons.[19]

The appropriate description of a photon has been discussed since the introduction of the word in 1926.[20] The mental picture that many students likely form when hearing the word photon is that of a small massless particle flying through space at the speed of light. In reality, quantized states of the radiation field involve excitations of spatial modes, which do not readily lend themselves to the mental pictures we form. It has been suggested that the word photon itself contributes to the widespread misunderstanding that surrounds the word and should therefore be eliminated.[21] The debate regarding how best to characterize a photon continues to this day.[22] Regardless of how it is described, experiments with single photons provide the simplest method to date for demonstrating the essential mystery of quantum mechanics.

Quantum optics experiments that address photon statistics and single-photon states have been incorporated into the undergraduate curriculum[23–25] and are one of the few ways students can easily observe a quantum-mechanical effect. The field has developed rapidly, thanks to technological advances and to the pioneering work of three groups.[26–31] Much of what we present here is motivated by these studies.

II. COUNTING STATISTICS, CORRELATIONS, AND LIGHT SOURCES

The primary goal of our sophomore-level class is for students to observe quantum-mechanical effects using single-photon states. Although detectors that can, in principle, measure single photons have existed for some time, we address two issues regarding this measurement. The first one is fundamental; a "click" registered at a detector does not necessarily imply a single photon was measured. As mentioned, a semiclassical theory predicts a similar pattern of clicks in the detectors. The second issue is technical; all detectors and their associated electronics have physical limitations such as efficiency and temporal resolution that affect the experimental results. We address both these issues in the following.

A. Radiation counting

Because single-photon experiments invariably rely on counting statistics and coincidence measurements, we begin with some counting experiments using radioactive sources. The students use an inexpensive handheld radiation sensor and a low-level source of radiation with a reasonably constant activity (half-life more than 1 month or so)[32] to perform several counting experiments that prompt a discussion of average, standard deviation, and standard deviation of the mean (standard error). In particular, students verify that a single experiment measuring N counts in T seconds has an average count rate of $\bar{R}=N/T$ with standard error $\sigma_{\bar{R}}\approx\sqrt{\bar{R}/T}$.[33]

The radioactive sample is next used as a source of uncorrelated events to investigate accidental coincidences. Two radiation sensors are placed next to each other a few inches in front of the source, while the count rates for each detector as well as the coincidence events are monitored. Radiation detectors, like single-photon detectors, convert an incoming "particle" to an electronic pulse. Although the output (temporal) pulse width τ depends on the type and quality of the detector, typical pulse widths range from tens of nanoseconds to milliseconds. For the counting circuit to register a coincidence, some portion of the pulse from the first detector must overlap with some portion of the pulse from the second detector. If the two detectors have the same pulse width τ, the total coincidence window is $\tau_c=2\tau$.[34]

For two random and independent sources, all coincidence counts are purely accidental. If the average count rates for the two detectors are R_1 and R_2, the expected rate of accidental coincidences is given by[35]

$$R_{\mathrm{acc}}^{(2r)}=\tau_c R_1 R_2=2\tau R_1 R_2. \tag{1}$$

The superscript $(2r)$ reminds us that $R_{\mathrm{acc}}^{(2r)}$ is the rate for twofold random coincidences. Because radioactive decay is a random process, the coincidence rate for two radiation detectors should be given, within statistical uncertainties, by Eq. (1).

Instead of quoting coincidence rates, it is convenient to introduce the "anticorrelation parameter" α defined by

$$\alpha\equiv\frac{P_c}{P_1P_2}, \tag{2}$$

where P_i is the probability of measuring a count in the ith detector and P_c is the probability of measuring a coincidence count. As its name suggests, the anticorrelation parameter provides a measure of how correlated the two sources are.[36]

To see its meaning more clearly, we write the probabilities in Eq. (2) in terms of measurable quantities. If the count rates are much smaller than the maximum possible count rates for the detectors, the probability of measuring an event is given by the number of measured events N, divided by the number of possible events N_p in a given time interval T, that is, $P=N/N_p$. In our experiment we measure both singles and coincidence counts. Experimentally, separate detectors are determined to be in coincidence if the output pulses overlap within the coincidence window τ_c. Therefore, the number of possible events is found by dividing the observation time by the coincidence window $N_p=T/\tau_c$. Substituting these probabilities into the anticorrelation parameter for two detectors gives

$$\alpha_{2d}=\frac{N_c}{N_1N_2}N_p=\frac{R_c}{\tau_cR_1R_2}=\frac{R_c}{R_{\mathrm{acc}}^{(2r)}}, \tag{3}$$

where we have used the fact that the average count rates are given by $R_i=N_i/T$. The $2d$ subscript indicates that the measurement involves two detectors.[37]

The two-detector anticorrelation parameter in terms of rates in Eq. (3) is seen to be the ratio of measured coincidences to the number of coincidences expected for random sources. This form of α_{2d} shows that correlated sources, which produce more coincidences than accidental, have $\alpha>1$. Similarly, anticorrelated sources, which produce fewer coincidences than accidental, have $\alpha<1$. As we will discuss, the classical description of light predicts $\alpha\geq1$, while a quantum description predicts $\alpha\geq0$. Thus, a measurement of $\alpha<1$ can be described only by a quantum theory of light.[19,39]

Not surprisingly, our measurements with radiation sensors give $\alpha=1$ (within statistical uncertainties). For our purposes, the main role of these experiments is to get students familiar with measuring pulse widths, understanding coincidence measurements, and calculating the anticorrelation parameter in a straightforward context.

B. Coincidence counting

In principle, coincidence measurements are very straightforward. The detector output signals are passed through a logical AND gate, and any overlap between the detector output pulses results in an output by the AND gate. There are two issues that complicate matters. First, we wish to reduce the pulse width from the detectors as much as possible. As shown in Eq. (1), reducing the pulse width cuts down on accidental coincidences. Second, we want the flexibility to measure different twofold and threefold coincidences at the same time.

The equipment often used to measure coincidences are time-to-amplitude converters, otherwise known as TACs. A TAC is a nuclear instrumentation module that is common in many physics departments. In addition to multiple TACs, multiple single channel analyzers (SCAs) and a nuclear instrumentation module bin are required. These units are a bit cumbersome for students to work with and cost many thousands of dollars if they are not already available. Furthermore, they have significant dead times that can lead to errors as the counting rates increase.[40] Although these errors can be corrected for, they present an added complication that distracts students from the primary focus of whether or not photons exist.

Fortunately, a low cost coincidence counting module has been developed just for this purpose.[41] We use the more recent field programmable gate array version of this module. After purchasing the programmable gate array board for around $300, it took only a few hours to load the program and get it working. The board takes four input signals and counts these signals and any four user-chosen coincidence combinations of the inputs. These data are output to a computer via a serial port (RS232) every tenth of a second, and a LABVIEW program controls the experiment time and processes the data. The user also has the option of shortening the widths of the input pulses. There are four choices ranging from no pulse shortening (in our case, ≈23 ns) down to a maximally shortened (≈4 ns) pulse width. More information on this coincidence counting module is available online.[42]

C. An incandescent point source of light

When transitioning from radioactivity to single-photon counting experiments, students will use optical equipment they may not have encountered before, including fiber optic cables, photon counting modules, and neutral density filters. To help ease this transition, it is useful to begin with an experiment that is qualitatively identical to the radioactivity experiment. This experiment also serves the purpose of allowing us to measure the coincidence window τ_c for our system. This information will be important when we measure the anticorrelation parameter for a helium-neon (HeNe) laser.

We begin by using a small incandescent light bulb as a point source of light; a "minimaglite" flashlight in candle mode is ideal. We treat this light as an incoherent source that emits light randomly in all directions[43] and is therefore analogous to the radioactivity experiment in terms of setup. Light is collected with two fiber-optic-coupled lenses (couplers) and sent to our light sensors. Because our ultimate goal is to demonstrate the existence of single photons, the light sensors must be extremely sensitive. We use a multichannel single-photon counting module (SPCM) produced by Perkin-Elmer (SPCM-AQ4C), which consists of four avalanche photodiodes. Because of the sensitivity and cost of the single-photon counting module, it is extremely important to ensure that any light entering the device is sufficiently dim by working in an appropriately darkened room and using neutral density filters whenever needed. In addition, placing 780 nm long-pass filters in-line with each channel of the module allows us to safely turn on lights that emit only visible wavelengths. A green LED lamp provides plenty of work light without affecting the detectors. Even with these filters in place, the minimaglite must be significantly dimmed with neutral density filters.[44]

One obvious feature of this experiment is that the count rate in each detector is not constant but fluctuates in a seemingly random manner. This behavior suggests to students that the light source is randomly emitting photons. However, the randomness of the detector outputs does not necessarily imply that the input to the detectors is random quantized packets. It is equally reasonable for (classical) electromagnetic waves to continually impinge on the detectors, which respond by randomly emitting single electrons that are amplified to produce clicks. The inability to distinguish between these two descriptions leads to one of the key points we make with our students: Because the predictions of the quantum and semiclassical theories are the same, we cannot distinguish between a random stream of photons and classical electromagnetic waves. This conclusion is important because it encourages students to think critically about what constitutes evidence for the photon.

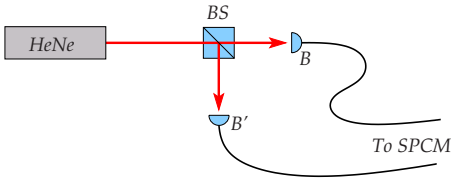

Fig. 1. The correlation experiment for a HeNe laser light source.

Following such a discussion, we perform one additional experiment with the incandescent light source. We use the random output pulses from the single-photon counting module to determine the coincidence window for our system. If we measure the number of coincidences as well as the single count rates in the two detectors, we can use Eq. (1) to determine τ_c. Because our coincidence counting module allows us to choose between four different pulse widths, we run four separate experiments to determine the coincidence window for each setting.

D. Statistics of laser light

After finding that light from an incandescent source is random in the sense that multiple detectors respond with random and uncorrelated clicks, we turn our attention to a light source that appears to be much less random, a HeNe laser. Using a laser allows us to make our first attempt at demonstrating the existence of photons. Because the laser emits light in a single direction, we insert a polarizing beam splitter into the beam path and direct the transmitted and reflected light into two optical fiber couplers labeled B and B' as shown in Fig. 1. A waveplate in front of the beam splitter allows us to adjust the polarization so that the measured amount of transmitted and reflected light is approximately the same. The coupler lenses can be aligned by eye while viewing the unconnected fiber output for transmission. Although the long-pass safety filters in front of the single-photon counting module have an optical density (at 632 nm) of approximately 10^5, a 1–10 mW laser still produces far more power than the single-photon counting module can handle.[45]

The experiment is simple to perform once the alignment and filtering are complete. The single-photon counting module has a maximum sustained count rate of around 10^6 counts per second (cps), so we aim for single count rates of less than 10^5 cps. Students measure the count rates in detectors B and B' as well as the BB' coincidences, and the anticorrelation parameter α_{2d} is then calculated using Eq. (3). Typical results for various coincidence windows are summarized in Table I where we report the averages of 25 5 s runs.[46] The values in parentheses give the uncertainty in the two rightmost digits as determined by the standard error.

Our results are consistent with $\alpha_{2d}=1$, which is expected if the detectors measure random and independent counts. This result suggests one of two possibilities. One option is that laser light consists of a random stream of quantized units (photons) that randomly reflect or transmit at the beam splitter, thereby causing the detectors to trigger randomly and independently. In this scenario, coincidences appear because

Table I. Correlation results for the transmitted and reflected channels of a HeNe laser through a beam splitter (rates in cps). We report averages of 25 5 s runs. $R_{\mathrm{acc}}^{(2r)}$ is calculated according to Eq. (1). The values in parentheses are the uncertainty in the rightmost digits as determined by the standard error.

τ_c (ns)	R_B	$R_{B'}$	$R_{BB'}$	$R_{\mathrm{acc}}^{(2r)}$	α_{2d}
45.51	43 280	43 640	85.4	86.0	0.993(07)
18.10	43 220	43 520	34.4	34.0	1.009(12)
12.31	43 110	43 370	22.5	23.0	0.977(24)
8.12	43 100	43 290	15.6	15.2	1.029(20)

there is always some chance that two (or more) photons appear very close together in time, one being transmitted while the other is reflected.

A second option is that the laser emits classical waves that divide equally at the beam splitter and impinge on the quantum-mechanical detectors, causing them to trigger randomly and independently as predicted by the semiclassical theory of radiation detection.[47] We stress to the students that a two-detector anticorrelation measurement of laser light cannot distinguish between a semiclassical and fully quantum-mechanical description of the light-matter interaction. Therefore, we are not justified in claiming that we have measured photons even though the detectors clearly trigger as individual events.

It is worth commenting further on this result. The fact that the measurement is consistent with a semiclassical theory comes about because the correct quantum-optical description of laser light above threshold is that of a coherent state, which is a superposition of photon number states with a Poissonian distribution.[10,48] Although quantum states, they correspond very closely to a classical description of electric fields,[49] and our measurement cannot distinguish between the two.

If we assume laser light is a Poissonian distribution of photon number states, our reduced-intensity laser beam is comprised predominately of single-photon states, even though $\alpha_{2d}=1$. For example, in the results shown in Table I, approximately 99.9% of the measurements result in singles as opposed to coincidences. Practically speaking, these results suggest that reduced-intensity laser light is a good single-photon source, a fact that has been utilized in simple experiments demonstrating interference and which-way information.[50,51] Nevertheless, because $\alpha_{2d}=1$ for laser light, these types of experiments are incapable of distinguishing between photons and classical electromagnetic waves, and hence we cannot yet claim we have detected a photon.

If we reduce the intensity further, we eventually reach the point where no coincidences are measured over an appreciable time (many seconds). Over this duration, $\alpha_{2d}=R_{BB'}/R_{\mathrm{acc}}^{(2r)}=0$, and we measure only single-photon states. The low count rates required to achieve this condition necessitate that the experiments be done over longer times, which leads to two problems. First, the single-photon counting module dark counts (those due to electronic noise and spurious light in the room) become important, complicating the analysis considerably. Second, running the experiment for longer times increases the chance of measuring a coincidence, resulting in a nonzero anticorrelation parameter. It turns out that when appropriately averaged over very long times, α_{2d} is always equal to one for a HeNe laser.

E. Spontaneous parametric down conversion

It is clear we need a different type of light source if we want to definitively demonstrate the quantum-mechanical properties of light. We use the process of type I spontaneous parametric down conversion, a nonlinear optical effect where light at a given frequency is converted into light of lower frequency.[52] Spontaneous parametric down conversion (hereafter referred to as down conversion) has become the standard method for generating quantum states of light.[53] Here, we provide only a brief overview of those aspects relevant to our experiments.

1. Down-conversion basics

Spontaneous parametric down conversion is not predicted classically and can be thought of as a quantum-mechanical process in which a single photon at frequency ω_1 is converted into two photons at frequencies ω_2 and ω_3 such that energy and momentum are conserved: $\omega_1=\omega_2+\omega_3$ and $\mathbf{k}_1=\mathbf{k}_2+\mathbf{k}_3$. (Although we have yet to demonstrate the existence of photons, we use the term throughout this section for simplicity.) Simply put, a single photon goes in and two photons come out simultaneously. Down conversion requires a nonlinear crystal, and due to momentum conservation in the crystal, the two lower-frequency photons exit in a cone about the input propagation axis. We use a blue diode laser ($\lambda=405$ nm) as the "pump" and choose the output "arms" in the same horizontal plane as the laser. Figure 2 shows a schematic of the experimental setup. Further details regarding the down-conversion process for these types of experiments can be found in Refs. 27 and 30.

The essential aspect of down conversion that permits observation of the quantum-mechanical properties of light is the correlation that exists between the two down-converted beams. Because each photon is in an energy superposition state and the total energy is fixed, the two photons are actually in an entangled state. Thus, a measurement of a photon in one arm provides, with absolute certainty, that a corresponding photon exists in the other arm at the same distance

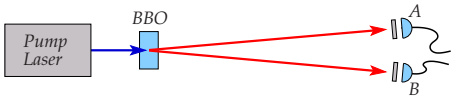

Fig. 2. A pump laser undergoes spontaneous parametric down conversion in a β-barium borate (BBO) crystal. The down-converted light is filtered before hitting the couplers. Although most of the pump laser passes unaffected through the crystal, we omit this beam from the diagram for clarity.

Table II. Correlation results for the two arms of our down-converted light source at two different count rates (all rates measured in cps). We report averages of 25 5 s runs. The values of the anticorrelation parameter indicate that the two arms are correlated (standard errors in parentheses).

τ_c (ns)	R_A	R_B	R_{AB}	$R_{\mathrm{acc}}^{(m)}$	$R_{\mathrm{acc}}^{(2r)}$	α_{2d}
45.51	45 720	45 620	1910	95.4	95.0	20.07(0.05)
18.10	45 730	45 670	1840	38.4	37.8	48.64(0.16)
12.31	45 720	45 670	1820	25.6	25.7	70.81(0.22)
8.12	45 700	45 670	1810	17.0	16.9	107.02(0.33)
45.51	11 350	11 300	414	6.00	5.83	71.1(0.3)
18.10	11 360	11 300	411	2.26	2.32	176.8(0.7)
12.31	11 370	11 320	412	1.60	1.59	259.6(1.2)
8.12	11 340	11 290	407	1.02	1.04	391.2(1.7)

from the crystal.[15] We refer to these two output photons as "twins," even though their energies are not necessarily equal.

In our experiment we use a β-barium borate (BBO) crystal cut at 29° so that the twin photons emerge with approximately equal energies ($\lambda=810$ nm) at 3° from the initial pump direction. The finite thickness (3 mm) of the crystal allows for a range of angles and wavelengths, and hence detector alignment is important and is performed before students enter the laboratory. The couplers are first set crudely in place using a ruler. A visible diode laser is shone back through the coupler and steered until it hits the center of the BBO crystal. This process typically aligns the coupler well enough to see the down-converted light in the single-photon counting module; the coupler is then tweaked to maximize the signal. The final adjustment is made using a 1 nm bandpass filter in front of the coupler. A similar procedure is used to align the second detector coupler, which is tweaked to maximize the coincidence signal. After the alignment is complete, we use 10 nm bandpass filters during the experiments to reduce the number of accidental coincidences.

2. Down-conversion correlations

Once in the laboratory, students perform a correlation measurement as before, except now the two detectors, A and B, measure counts in both arms of down-converted light. Because the beams are correlated, we expect the number of measured coincidences to be greater than those of a random source, that is, $\alpha_{2d}>1$. Typical results from 25 5 s runs are summarized in Table II.

The most obvious feature of the data in Table II is that α_{2d} is larger than one, indicating the down-converted light is correlated. Because in theory the two arms are perfectly correlated, it might be surprising that α_{2d} is not found to be even larger. To understand why, we consider an ideal experiment with perfect coupler alignment, perfect detectors, and no background noise. In this case every twin pair produced by the down-conversion crystal will be measured by both detectors and all of these pairs will be in perfect coincidence. Therefore, if the rate of twins incident on the detectors is $R^{(t)}$, then $R_A=R_B=R_{AB}=R^{(t)}$, and α_{2d} is given by

$$\alpha_{2d}=\frac{R_{AB}}{\tau_c R_A R_B}=\frac{1}{\tau_c R^{(t)}}. \tag{4}$$

For typical singles rates of 10^4 cps and $\tau_c=8$ ns, we would measure $\alpha_{2d}=12\,500$. In reality, the overall efficiency of our system, including the optics, alignment, and detector, is around 4% (see Appendix A for details). Such a small efficiency tells us that the twin production rate must be about 25 times higher than our measured singles rates, resulting in an anticorrelation parameter of at most ~500, in rough agreement with our measurements. A more careful analysis is carried out in Appendix A.

Interestingly, α_{2d} can be increased by decreasing the number of twins, a behavior born out in Table II. Although such an increase seems counterintuitive, it is merely an indication that the accidental coincidence rate depends quadratically on $R^{(t)}$, while the measured coincidence rate depends linearly on $R^{(t)}$.

3. Accidental coincidences

Another obvious feature in Table II is that the coincidence counts are not constant as we decrease the coincidence window despite the fact that perfectly correlated twin coincidences should not depend on τ_c. This suggests that a portion of our measured coincidences is accidental. Depending on the amount of filtering and how carefully the detector couplers have been aligned, these accidental coincidences may or may not account for a substantial percentage of the measured coincidences.

Fortunately, it is straightforward to measure the number of accidental coincidences. Because the down-conversion process is random and the twins occur simultaneously, we delay the output of one channel of the single-photon counting module so that a twin pair no longer triggers a coincidence. This delay is accomplished by inserting a longer coaxial cable between the output of one channel of the single-photon counting module and the counter. Because this shift does not affect the (average) count rate of accidental coincidences, the net effect is to eliminate the twin coincidences and leave only the accidentals. These measured accidentals are displayed as $R_{\mathrm{acc}}^{(m)}$ in Table II (the superscript denotes that these are measured accidentals). When these accidentals are accounted for, the rate of real (twin) coincidences is found to be independent of the coincidence window.

As the data in Table II show, the accidental coincidence counts can be made negligibly small by reducing the overall count rate or by reducing the coincidence window. Eliminating accidental coincidences obviates the need for a lengthy discussion of their cause. Nevertheless, it can be instructive to at least discuss qualitatively how such accidentals arise. Such a discussion and a detailed analysis of the accidental coincidences are given in Appendix A. The result is that the rate of expected accidentals is approximately given by the twofold accidental coincidence rate

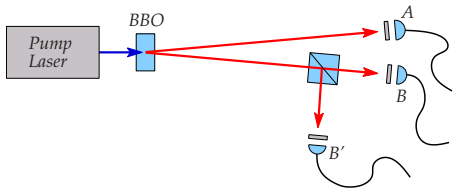

Fig. 3. The three-detector correlation experiment using a light source derived from spontaneous parametric down conversion.

$$R_{\mathrm{acc}} \approx R_{\mathrm{acc}}^{(2r)} = \tau_c R_A R_B. \tag{5}$$

As shown in Table II, this twofold accidental coincidence rate agrees with the measured accidentals.

We emphasize that the down-converted light can be thought of as two perfectly correlated streams of random photons as can be confirmed by sending one arm, say, the B line, into a beam splitter and measuring the anticorrelation parameter for the transmitted and reflected beams (B and B'). Just as with the HeNe experiment, we find $\alpha_{2d}=1$. Thus, we still do not have a light source that unequivocally demonstrates the existence of photons. To accomplish this, we must exploit the correlated properties of this light source to reveal its true quantum-mechanical nature.

III. PHOTON QUANTUM MECHANICS

A. Photons at last

Because the two arms of down-converted light are perfectly correlated, the measurement of a photon in one arm guarantees the existence of a photon in the other. This source is often called a "heralded" single-photon source because one photon announces the arrival of the other. Knowing exactly when there is a photon in the second arm is the key to this experiment. The arrangement is nearly the same as the experiment with the HeNe laser. The B line of the down-converted light enters a beam splitter, while the A line goes directly to a single detector (see Fig. 3). When detector A is triggered, we know there is a photon at the beam splitter in the B line. Thus, we perform a correlation experiment between B and B', conditioned on a measurement at A.

The probabilities used to calculate the anticorrelation parameter between B and B' must now be found in reference to the counts N_A in the A arm. Specifically, the number of possible events is now N_A (these are the only times we look at the B and B' detectors) compared to T/τ_c as we had in the two-detector situation. This large decrease in the number of possible events leads to a dramatic increase in the probabilities—knowing precisely when to look means we are much more likely to detect an event. Increasing the probabilities in Eq. (2) in turn leads to a decrease in the anticorrelation parameter.

Quantitatively, the probability of measuring a count at B (conditioned on A) is

$$P_B = \frac{N_{AB}}{N_A}, \tag{6}$$

where N_{AB} is the number of AB coincidence counts. A similar expression holds for $P_{B'}$. The conditional probability for measuring BB' coincidence counts is

$$P_{BB'} = \frac{N_{ABB'}}{N_A}, \tag{7}$$

where $N_{ABB'}$ is the number of ABB' triple coincidences. We combine these probabilities as in Eq. (2) and express the anticorrelation parameter in terms of measurable quantities as

$$\alpha_{3d} = \frac{N_{ABB'}}{N_{AB}N_{AB'}}N_A = \frac{R_{ABB'}}{R_{AB}R_{AB'}}R_A, \tag{8}$$

where we have written α_{3d} to signify that this measurement involves three detectors.

Once the beam splitter is in place,[54] the experiment is straightforward. We measure the appropriate coincidence rates and calculate according to Eq. (8). Because a semiclassical theory of light predicts $\alpha \geq 1$, a measurement of $\alpha < 1$ is an indication that the source must be treated quantum mechanically. In brief, measuring α less than one demonstrates the existence of photons. The closer α is to zero, the closer we are to having a single-photon source.

Typical results are shown in Table III. We find $\alpha < 1$, which provides clear evidence for the quantum nature of light. This result tells us that light consists of quanta that can either be transmitted or reflected at a beam splitter, but never both. This result is worth emphasizing to students because later we will show that such light quanta can travel both ways at a beam splitter but only if it is impossible to determine which way the photon travels.

Table III. Correlation results for a three-detector measurement using a down-converted light source (all rates measured in cps). We report averages of 25 5 s runs. Although not shown, R_B and $R_{B'}$ are approximately the same as R_A. The values in parentheses are the uncertainties in the rightmost digit as determined by the standard error.

τ_c (ns)	R_A	R_{AB}	$R_{AB'}$	$R_{ABB'}$	R_{acc}^{3d}	α_{3d}
45.51	45 300	1750	1470	6.38	6.6	0.113(5)
18.10	45 280	1690	1400	2.18	2.5	0.042(2)
12.31	45 340	1660	1390	1.64	1.7	0.032(2)
8.12	45 310	1660	1390	0.91	1.1	0.018(1)
45.51	15 350	536	446	0.78	0.71	0.050(5)
18.10	15 350	528	443	0.18	0.28	0.012(3)
12.31	15 360	526	436	0.20	0.19	0.014(3)
8.12	15 350	524	432	0.09	0.12	0.006(2)

B. Estimating three-detector accidentals

A true single-photon source[55] would yield $\alpha_{3d}=0$. Because we do not measure α_{3d} to be identically zero, it is clear from Eq. (8) that $R_{ABB'}$ cannot be zero. In other words, we must be measuring some threefold coincidences. Here, we estimate the number of accidental threefold coincidences we expect to find in this experiment.

One possibility is for three uncorrelated photons to end up at detectors A, B, and B' within a small enough time such that the pulses overlap. However, for small pulse widths, such threefold random accidentals are extremely rare because this rate depends on the square of τ: $R_{\mathrm{acc}}^{(3r)}=3\tau^2 R_A R_B R_{B'}$.[35] A quick calculation shows that $R_{\mathrm{acc}}^{(3r)}$ is approximately two orders of magnitude less than the measured rate.

Much more likely is a twofold random accidental between a real AB coincidence and a random B' single (or similarly, between a real AB' coincidence and a random B single). The threefold accidentals are dominated by such coincidence/single events. When background and nontwin events are negligible (see Appendix A), the coincidence/single events are easy to calculate with the help of Eq. (1), which gives

$$R_{\mathrm{acc}}^{3d} \approx \tau_c (R_{AB} R_{B'} + R_{AB'} R_B). \tag{9}$$

The approximate threefold coincidence rates as calculated by Eq. (9) are shown in Table III. The agreement between theory and experiment gives us confidence that these accidentals account for essentially all of the measured ABB' coincidences and explains why the anticorrelation parameter is not exactly zero.

If we want to improve our correlation measurement, we must reduce these accidental coincidences. From Eq. (9) it is clear that one way to do so is to reduce the coincidence window as much as possible. Although this procedure is supported by the data in Table III, the coincidence window is ultimately limited by hardware and can only be reduced so far. As discussed more fully in Appendix B, a more effective way to reduce α is by reducing the twin production rate. This reduction is accomplished by reducing the power of the pump laser, which effectively lowers all of the count rates in Eq. (9). This effect can be seen in Table III and more clearly in Fig. 6.

Interestingly, down-converted light is similar to "normal" laser light in that lower count rates are needed to keep the likelihood of multiphoton states to a minimum. Using a down-conversion light source as described here is often referred to as a "pseudo-single-photon source" because the maximum count rate must be limited. This requirement is in contrast to microscopic single-photon sources that have negligible multiphoton probabilities at comparable brightness.[55] Although similar in some ways, a fundamental difference between dim laser light and down-converted light is that for sufficiently low count rates, the average value of α_{3d} for down-converted light is much less than one, a result that is inconsistent with a classical description of light.

C. Interference of single photons

With this pseudo-single-photon source, we can now perform experiments that exhibit the essential mystery of quantum mechanics (dubbed complementarity by Niels Bohr). Because these experiments have been well described,[27] we provide only an overview. We construct a Mach–Zehnder interferometer with nonpolarizing beam splitters, a path length of about 30 cm, and a movable, piezocontrolled mirror (see Fig. 4). Single photons, as determined by continuously measuring an anticorrelation parameter less than one, are then directed into the interferometer. Because these photons spend no more than 1 ns in the interferometer and are separated by at least 4 ns (using our smallest pulse width setting), we guarantee that only single photons inside the interferometer contribute to our measurements.

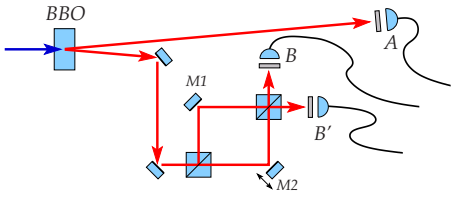

Fig. 4. Two steering mirrors guide one arm of the down-converted light into a Mach–Zehnder interferometer with movable mirror $M2$. By using detectors A, B, and B', we continually monitor α_{3d} to verify single photons in the interferometer.

As mirror $M2$ is moved by a few microns, the conditioned counts in B and B' exhibit interference fringes. We stress to students that these interference fringes depend on the path length difference between the two arms of the interferometer. Because the interference pattern is constructed from single photons, our conclusion is that each photon must somehow "sample" both paths of the interferometer. Precisely how this sampling occurs, of course, is the central mystery of quantum mechanics.

Although other interferometers exist that are simpler to align,[31] we use a Mach–Zehnder for three main reasons. First, our students have experience constructing such an interferometer with a HeNe laser in a previous course, and although the alignment using down-converted light is more challenging and done by the instructor, their experience makes this portion of the experiment easy to understand. Second, a Mach–Zehnder interferometer presents an obvious physical separation between the two arms that helps maximize the impact of the experimental results; how can a single photon be in two places at once? Third, there is a well-defined procedure for aligning a Mach–Zehnder interferometer that makes the process painless,[56] even though the path lengths of the two arms must be equal to within the coherence length of our source ($\approx$65 μm when using 10-nm filters).[57]

Typical results for this experiment are plotted in Fig. 5, which shows the conditioned counts in the B detector as a function of the scaled path length difference $\Delta l/\lambda$ between the two arms. The conditioned B' counts (not shown) are 180° out of phase with the B counts. The fringe visibility, which is used to quantify the quality of the interference pattern, is defined as

$$V = \frac{R_{\max} - R_{\min}}{R_{\max} + R_{\min}} \tag{10}$$

and is 94% in this case. Because the interferometer is sensitive enough to be affected by vibrations and air currents, experimental errors are not necessarily dominated by statistical fluctuations. The error bars in Fig. 5 represent the measured standard deviations. The error bars for the "tagged" and "erased" photons (described in the following) are ap-

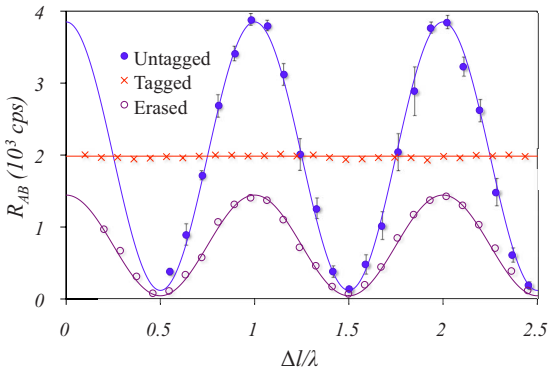

Fig. 5. Conditioned count rate as a function of the (scaled) path length difference for single photons in a Mach–Zehnder interferometer. Interference is observed when photons are "untagged" (filled circles) but is not observed when photons are tagged (crosses). Interference returns when a polarizer erases the path information (open circles). The smooth curves are the predictions given by Eq. (21).

proximately the size of the markers and have been eliminated for clarity.

The interference pattern depends on both paths in the interferometer. Because only single photons are ever present, each photon somehow "knows" about both paths of the interferometer—it appears to travel both ways at the same time. But how is this possible when our earlier experiment demonstrated that photons incident on a beam splitter are either transmitted or reflected but never both? To answer this question, we look carefully at the difference between the two experiments. In the first case the detectors are placed after a single beam splitter, allowing us to determine whether each photon is transmitted or reflected. But in the interferometer experiment, the detectors are placed after the two paths have been recombined on a second beam splitter. Therefore, we can no longer determine whether each photon was transmitted or reflected at the first beam splitter. This difference is crucial.

To emphasize this point we now "tag" each photon by altering the polarization in one arm of the interferometer. This is accomplished by using half waveplates in both arms of the interferometer. With orthogonal polarizations each photon carries information that unambiguously determines which way it travels in the interferometer. If we know with certainty that each photon takes one and only one path through the interferometer, it is impossible for there to be an interference pattern.[58] Sure enough, repeating the experiment while scanning the mirror results in no interference fringes (see Fig. 5).

We can "erase" the path information by placing a linear polarizer in one of the output ports of the Mach–Zehnder interferometer. This polarizer is oriented at 45° to the two polarizations so that every photon has a 50% chance of being transmitted. Transmitted photons all have the same polarization, and it is therefore impossible to determine which path they take through the interferometer. When repeating the experiment in this configuration, the interference pattern returns as shown in Fig. 5.[59] The fact that the amplitude has decreased by more than a factor of two is due to the fact that our linear polarizer is only about 75% efficient for light polarized along the transmission axis.

Lastly, we describe an experiment that dramatically illustrates the quantum-mechanical nature of our experimental setup. As mentioned, interference fringes are observed only if the two path lengths in the Mach–Zehnder interferometer are equal to within the coherence length of our light source. We can move mirror $M2$ so that the path length difference is well beyond this coherence length. With no bandpass filters, a 40 μm path length difference gives no interference fringes when the mirror is scanned through a few microns. The fringes return if we place a 1 nm bandpass filter in front of the A detector (thereby increasing the coherence length of light in the A arm), even though no direct changes were made to the light traversing the interferometer.

The (orthodox) quantum-mechanical description of this experiment is as follows. Because the two down-converted photons are in an energy-entangled state, measuring the wavelength (energy) in the A-line collapses the wave function so that the wavelength (energy) is now determined in the interferometer as well. Although there are other descriptions that explain these results, this nonlocal description provides students with some of the background they will need to understand Bell's theorem. The experimental setup described in this section can be easily modified to test for violations in Bell's inequalities.[60] We are currently working on such experiments for use in our upper-level quantum mechanics course.

D. Quantum-mechanical predictions

The experiments we have described are used with second-year physics majors, and thus a formal treatment of quantum mechanics is beyond the scope of the course. Nevertheless, we want these students to learn the basic skills necessary to calculate quantum-mechanical probabilities for simple situations. Thus, we spend much time discussing two-state spin systems and Stern–Gerlach experiments as described in Ref. 61. As is becoming more common in elementary treatments of quantum mechanics, this text uses bra-ket notation. Although this notation is unfamiliar and a bit exotic for these students, that is precisely one of its pedagogical advantages. In quantum mechanics the interpretation is dramatically different from classical mechanics, and we find that this notation helps students understand that we are dealing with something unlike anything they have seen before.

Because of the mathematical similarities, our Mach–Zehnder interferometer experiments can be elegantly described using a similar approach to Stern–Gerlach experiments. The advantage is that our students have done these experiments themselves. We hope that when students are able to compare their calculations to their experimental results, they will begin to see quantum mechanics as being "real" and concrete rather than mystical and confusing.

Our approach is similar in spirit to those in Refs. 26, 27, and 62. Although the mathematics is the same as if we were treating light classically, the fact that our experiments happen one photon at a time forces us to interpret the equations in a completely different manner. This interpretation gives these calculations their quantum-mechanical "feel." In the following, we outline the calculations our students work through, beginning with a simple beam splitter and ending with the quantum eraser.

1. A beam splitter

Suppose we send a photon into a beam splitter and ask whether the photon is transmitted or reflected. Quantum me-

chanics says we cannot determine the answer to this question in advance. Instead, we can only predict the probability of observing each outcome. We represent the input state, which consists of a single photon entering one input port of the beam splitter and zero photons entering the other input port, by $|\psi_{\text{in}}\rangle$. There are two possible output states: A single photon reflected and zero photons transmitted, represented by $|\psi_R\rangle$, and a single photon transmitted and zero photons reflected, represented by $|\psi_T\rangle$. These output states are eigenstates of the number operator. For our purposes the important point is that these two output states can be used as an orthonormal basis.

Quantum mechanics tells us that there is a (complex) probability amplitude associated with going from the input state to each of the two output states.[58] We write these amplitudes as $r=|r|e^{i\phi_r}$ for reflection and $t=|t|e^{i\phi_t}$ for transmission. Our input state is then transformed by the beam splitter according to

$$|\psi_{\text{in}}\rangle \rightarrow r|\psi_R\rangle + t|\psi_T\rangle. \tag{11}$$

The probability of finding the photon in state $|\psi_R\rangle$ (reflected) is $P_R=|\langle\psi_R|\psi_{\text{in}}\rangle|^2=|r|^2\equiv R$, and the probability of finding it in state $|\psi_T\rangle$ (transmitted) is $P_T=|\langle\psi_T|\psi_{\text{in}}\rangle|^2=|t|^2\equiv T$. Here, R and T are the reflection and transmission probabilities for this input port of the beam splitter. A lossless beam splitter has $R+T=1$ because the photon must be found somewhere.

2. A simple Mach–Zehnder interferometer

Now suppose we send a photon into a Mach–Zehnder interferometer with equal and fixed path lengths. The input state is still labeled as $|\psi_{\text{in}}\rangle$, and $|\psi_R\rangle$ and $|\psi_T\rangle$ now represent the intermediate states of the interferometer. The output states, which are used as an orthonormal basis, are represented by $|\psi_B\rangle$ and $|\psi_{B'}\rangle$ according to whether the photon travels toward detector B or B', respectively (see Fig. 4). Because each path through the interferometer has a single mirror and equal path lengths, any phase contributions from these two paths are identical and can safely be ignored (for now).

The second beam splitter transforms each of the intermediate states in the interferometer. For a symmetric beam splitter (one that has identical reflection and transmission properties for both input ports), we find

$$|\psi_R\rangle \rightarrow r|\psi_B\rangle + t|\psi_{B'}\rangle \tag{12}$$

and

$$|\psi_T\rangle \rightarrow t|\psi_B\rangle + r|\psi_{B'}\rangle. \tag{13}$$

Upon substitution into Eq. (11), we find the probability that a photon arrives at detector B is

$$P_B = |\langle\psi_B|\psi_{\text{in}}\rangle|^2 = R^2 + T^2 + 2RT\cos[2(\phi_r - \phi_t)], \tag{14}$$

and the probability that a photon arrives at B' is

$$P_{B'} = |\langle\psi_{B'}|\psi_{\text{in}}\rangle|^2 = 4RT. \tag{15}$$

For lossless beam splitters the sum of these probabilities must be unity, which, with $R+T=1$, constrains the phases of the reflection and transmission amplitudes to satisfy

$$\phi_r - \phi_t = \pm\,\pi/2. \tag{16}$$

3. Interference in a Mach–Zehnder interferometer

As our first example of interference, we consider the more general Mach–Zehnder interferometer where the two path lengths are not exactly equal. When the photon arrives at the second beam splitter, the intermediate state wave functions will have acquired an extra phase factor, which depends on the distance traveled. Let ℓ_1 represent the distance traveled in state $|\psi_R\rangle$ and ℓ_2 the distance traveled in state $|\psi_T\rangle$. Then the right-hand sides of Eqs. (12) and (13) pick up phase factors of $e^{i\delta_1}$ and $e^{i\delta_2}$, respectively, where $\delta_i=2\pi\ell_i/\lambda$. We follow the same procedure as before, make use of Eq. (16), and take $R=T=1/2$ to find

$$P = \tfrac{1}{2}(1 \mp \cos\,\delta), \tag{17}$$

where $\delta=\delta_2-\delta_1$ and the upper (lower) sign gives the probability that a photon arrives at detector B (B'). These probabilities display the characteristic interference fringes as a function of path length difference between the two arms of the interferometer. Because single photons are traveling through the interferometer, the conclusion is that each photon must "take both paths," making this a natural place to qualitatively describe Feynman's sum-over-paths approach to quantum mechanics.[64] When going from an input state to an output state, a photon, or any other quantum object, takes "all possible paths" that are available. To correctly calculate the probability, we must sum the amplitudes for every possible path and square the result.

Because it seems preposterous to students that a particle can take multiple paths through the Mach–Zehnder interferometer, we next propose to tag the photons by giving each intermediate path in the interferometer an orthogonal linear polarization. We do so by using half waveplates in each arm of the interferometer. In our experiment the waveplates are oriented so that photons reflected at the first beam splitter remain vertically polarized, while photons transmitted are horizontally polarized. Thus, in addition to the path length phase factors, the right-hand sides of Eqs. (12) and (13) pick up polarizations $|V\rangle$ and $|H\rangle$. With $R=T=1/2$, we find the probabilities for arriving at detectors B and B' to be

$$P_B = P_{B'} = \tfrac{1}{2}. \tag{18}$$

Lastly, we need to describe how the addition of a polarizer outside the interferometer brings back the interference fringes. The action of a linear polarizer with its transmission axis at an angle θ with respect to the vertical is described by the projection operator $|T_\theta\rangle=\cos\,\theta|V\rangle+\sin\,\theta|H\rangle$. That is, the probability that a photon in polarization state $|\psi_p\rangle$ passes through the polarizer is given by $|\langle T_\theta|\psi_p\rangle|^2$. In our experiment, photons exiting the Mach–Zehnder interferometer toward detector B are in the (polarization) state

$$|\psi_p\rangle = r^2 e^{i\delta_1}|V\rangle + t^2 e^{i\delta_2}|H\rangle. \tag{19}$$

For $\theta=-\pi/4$ the probability that such a photon will pass through the polarizer is[63]

$$P_B = \tfrac{1}{4}(1 - \cos\,\delta), \tag{20}$$

where we have used Eq. (16) and set $R=T=1/2$. Note that Eq. (20) is half of our original interference result given in Eq. (17), which is what we would expect for a perfect polarizer. In reality, our linear polarizer has an efficiency of 75%, and therefore Eq. (20) must be appropriately modified when comparing to experiments.

The data shown in Fig. 5 were taken at detector B so that the applicable predictions are given by Eqs. (17), (18), and (20). These predictions give probabilities, while the experiments are measured in counts per second; thus they cannot be directly compared. In addition, it is very difficult to align the interferometer to obtain perfect fringe visibility. To account for these experimental imperfections, the data are modeled using the expression

$$R_{\text{avg}}(1 - V\cos\delta), \tag{21}$$

where R_{avg} is the average count rate and V is the fringe visibility defined in Eq. (10). Equation (21) is used to model the data and is displayed as solid curves in Fig. 5 with $R_{\text{avg}}=1,985$ and $V=0.94$ or $V=0$. The erased prediction is further multiplied by 0.75 to account for the polarizer efficiency. The agreement between theory and experiment is impressive, particularly to students who have labored over the experiments and calculations.

IV. CONCLUSIONS

We have described a series of experiments that have been adapted for use in our second-year quantum physics class. These experiments provide students the opportunity to witness the counterintuitive behavior of quantum phenomena in a hands-on setting. The associated calculations give students a brief introduction to quantum theory in a way that is directly connected to the experiments. This connection helps students see the "big picture" behind quantum theory and reduces the confusion that often accompanies a more advanced course in quantum mechanics.

Although we are in the early stages of development, the material presented here was classroom tested in the Spring of 2009. Our formative assessments have focused almost solely on student attitudes, and we can report that students were extremely enthusiastic about these experiments. This enthusiasm seemed to motivate the students to really want to understand the theory behind the experiments. In the future we hope to quantify these student attitudes and begin to probe if students are actually learning this material as well as it seems.

Incorporating these experiments into the curriculum took a substantial investment of time and money. Some of the equipment took a month or more to arrive, and it can require several weeks just to get items unpacked and properly set up. Once everything is assembled, the experiments themselves might take a few weeks to get working satisfactorily. We opted to have four physics majors set up these experiments as part of a senior project. None of them had any optics experience, and thus we included some simple optics experiments to give them the relevant background they would need. Ultimately, it took the students about a full semester to get things working reliably.

Although there have been several articles published on this topic, we have tried to elaborate on many of the details that we found confusing when implementing these experiments. We have also attempted to include a reasonably complete account of what we present to our students. Incorporating these experiments into our curriculum has been a rewarding endeavor for the faculty and students involved, and we hope this presentation will motivate others to incorporate similar experiments into the undergraduate curriculum.

ACKNOWLEDGMENTS

The authors gratefully acknowledge the technical expertise and assistance of Enrique "Kiko" Galvez of Colgate University and Mark Beck of Whitman College. We also acknowledge useful discussions with our colleagues at Dickinson College. The authors would like to thank an anonymous reviewer for helpful comments and a prompt and thorough reading of our manuscript. This project was supported by the National Science Foundation under Grant No. DUE-0737230 with additional funding provided by Dickinson College.

APPENDIX A: ACCIDENTAL COINCIDENCE RATE FOR A SPONTANEOUS PARAMETRIC DOWN-CONVERSION LIGHT SOURCE

In this appendix we consider more closely the accidental coincidence rate for the spontaneous parametric down-conversion experiment described in Sec. II E. There are three main sources of accidental coincidences in this experiment. The first is due to detector inefficiency. In an ideal experiment, the only light that enters the detectors are twins from the down-conversion crystal, which means that each photon incident on detector A has a twin that is simultaneously incident on detector B. Because the single-photon counting module is not 100% efficient and many photons are lost in the optical elements (filters and fiber cables), when a photon is measured at detector A, there is a good chance that the twin photon appearing at detector B will not be measured. If only one of a twin pair is measured at A and only one of a separate twin pair is measured at B, there is a chance that these two events will give rise to an accidental coincidence.

Another cause of accidentals is due to the misalignment of the detector couplers. It is almost impossible to align the two detectors so that they see exactly the same bandwidth from the crystal. Thus, in addition to twin pairs incident on the detectors, there will be "nontwins" coming from the crystal that are incident on the detectors. The third cause of accidentals is what we call background, which consists of "dark counts" from within the detector plus any stray light that enters the detectors that is not generated in the crystal. All of these sources are assumed to be random.

We denote the rate of twins measured by detectors A and B to be $R_A^{(t)}$ and $R_B^{(t)}$, respectively. Although the number of twins emanating from the crystal toward the detector couplers is exactly the same (by definition), the number of twins actually measured by the detectors will not be the same because each detector and accompanying optics have a different overall efficiency. This efficiency is the probability that a down-conversion photon produced by the crystal and in the appropriate solid angle (that is, traveling toward the detector coupler) is actually measured by the detector. We denote these efficiencies as η_A and η_B so that

$$R_A^{(t)} = \eta_A R^{(t)} \quad \text{and} \quad R_B^{(t)} = \eta_B R^{(t)}, \tag{A1}$$

where $R^{(t)}$ is the average rate of twins traveling from the crystal toward the detector couplers.

Similarly, we denote the measured rate of nontwins and background counts by $R_A^{(\text{nt})}$, $R_B^{(\text{nt})}$, $R_A^{(\text{bg})}$, and $R_B^{(\text{bg})}$. In theory, the background counts can be measured by closing the alignment irises. Usually the rate of twins or nontwins emanating from the crystal is much higher than the background rates unless the count rates have been purposely reduced. For ex-

ample, we measure background rates of approximately 1000 cps in our experiments (see Tables II and III).

Having accounted for all sources of light in the detectors, the measured count rates are given by

$$R_A = \eta_A R^{(t)} + R_A^{(nt)} + R_A^{(bg)} \tag{A2}$$

and

$$R_B = \eta_B R^{(t)} + R_B^{(nt)} + R_B^{(bg)}. \tag{A3}$$

The measured coincidence rate is given by the sum of real plus accidental coincidences

$$R_{AB} = R_{AB}^{(real)} + R_{AB}^{(acc)}. \tag{A4}$$

Real coincidences are found by multiplying the twin rate by the probabilities that each detector will trigger

$$R_{AB}^{(real)} = \eta_A \eta_B R^{(t)}. \tag{A5}$$

To find the rate of accidental coincidences, we rely again on the twofold random coincidence expression in Eq. (1), subject to the condition that R_1 and R_2 (R_A and R_B in our experiment) represent the measured count rates, not including any real coincidences. Thus, we need to subtract the rate of real coincidences from the measured rates R_A and R_B (Ref. 65) to get

$$R_{AB}^{(acc)} = \tau_c (R_A - \eta_A \eta_B R^{(t)})(R_B - \eta_A \eta_B R^{(t)}). \tag{A6}$$

When Eqs. (A5) and (A6) are substituted into Eq. (A4), we are left with three equations, (A2)–(A4), and five unknowns ($R_A^{(nt)}$, $R_B^{(nt)}$, η_A, η_B, and $R^{(t)}$). These equations cannot be solved without additional information. However, we can infer from Eq. (A6) that the expected accidental coincidence rate is always less than the twofold random rate, and for low efficiencies they are approximately equal

$$R_{AB}^{(acc)} \approx \tau_c R_A R_B. \tag{A7}$$

As we will demonstrate, our efficiencies are typically under 5%, making Eq. (A7) an excellent approximation. To say anything more requires that we make certain assumptions about the system. Two situations warrant further investigation.

1. Perfect coupler alignment

Here we assume the detector couplers are nearly perfectly aligned so that twin events dominate nontwin events. This is the situation we seek to attain in the laboratory. In practice, aligning the detectors perfectly is almost impossible. However, using narrow-band filters limits the spectrum reaching the detectors so that twin events will dominate even for imperfect coupler alignment. In such a scenario, we have

$$R_A \approx \eta_A R^{(t)} + R_A^{(bg)} \tag{A8}$$

and

$$R_B \approx \eta_B R^{(t)} + R_B^{(bg)}, \tag{A9}$$

which when combined with Eqs. (A4)–(A6) give three equations with three unknowns. Although these equations can be solved exactly, the results are cumbersome and not enlightening. Nevertheless, given measurements of R_A, R_B, $R_A^{(bg)}$, $R_B^{(bg)}$, and R_{AB}, we can numerically determine η_A, η_B, and $R^{(t)}$. For the data in Table II, we find $\eta_A \approx 4.05\%$, $\eta_B \approx 4.05\%$, and $R^{(t)} \approx 1.10 \times 10^6$ cps for the higher-count-rate data and $\eta_A \approx 3.99\%$, $\eta_B \approx 4.01\%$, and $R^{(t)} \approx 2.56 \times 10^5$ cps for the lower-count-rate data.

Given such low efficiencies, Eq. (A7) is a valid approximation. This allows us to solve Eqs. (A7)–(A9) analytically to find the efficiencies and the twin rate in terms of easily measurable quantities. The results are

$$\eta_A \approx \frac{\tilde{R}_{AB}}{\tilde{R}_B}, \quad \eta_B \approx \frac{\tilde{R}_{AB}}{\tilde{R}_A}, \tag{A10}$$

and

$$R^{(t)} \approx \frac{\tilde{R}_A \tilde{R}_B}{\tilde{R}_{AB}}, \tag{A11}$$

where $\tilde{R}_A = R_A - R_A^{(bg)}$, $\tilde{R}_B = R_B - R_B^{(bg)}$, and $\tilde{R}_{AB} = R_{AB} - \tau_c R_A R_B$ are the real (in contrast to measured) rates. This set of equations yields results that are almost identical to the numerical results quoted following Eq. (A9) and are far simpler to use.

The equations simplify further when the background rates and accidental coincidences can be neglected. In this case we have the relations

$$R_A \approx \eta_A R^{(t)}, \quad R_B \approx \eta_B R^{(t)}, \tag{A12}$$

and

$$R_{AB} \approx \eta_A \eta_B R^{(t)}, \tag{A13}$$

which are seen frequently in the literature.[66] From an educational perspective Eqs. (A12) and (A13) are simple to understand from first principles because they only make use of twin events and system efficiencies. They are easily solved to give

$$\eta_A \approx \frac{R_{AB}}{R_B}, \quad \eta_B \approx \frac{R_{AB}}{R_A}, \tag{A14}$$

and

$$R^{(t)} \approx \frac{R_A R_B}{R_{AB}}. \tag{A15}$$

By using the data in Table II, we find $\eta_A \approx 4.04\%$, $\eta_B \approx 4.03\%$, and $R^{(t)} \approx 1.13 \times 10^6$ for the higher-count-rate data. These values compare favorably with the numerical results calculated following Eq. (A9). For the lower-count-rate data, we find $\eta_A \approx 3.64\%$, $\eta_B \approx 3.62\%$, and $R^{(t)} \approx 3.12 \times 10^5$. The fact that the lower-count-rate data do not agree as well with the earlier numerical results should not be a surprise. In this case we have neglected background events, which account for a substantial portion ($\approx 10\%$) of the singles counts.

The anticorrelation parameter can be calculated using Eqs. (A12) and (A13), and the result is the same as for a perfect experiment, $\alpha = 1/(\tau_c R^{(t)})$.

2. A "noisy" system

Because the bandpass filters prevent some of the down-converted light from entering the detector couplers, they reduce the total efficiency of our system. Thus, we might expect our experimental results to improve if we remove the filters after aligning the system. To test this idea, we perform an identical set of experiments as described in Sec. II E. The only difference is that the bandpass filters are removed. The results are shown in Table IV.

Table IV. Correlation results for the two arms of our down-converted light source with no bandpass filters in front of the detector couplers (all rates measured in cps). We report averages of 25 5 s runs. The values in parentheses are the uncertainty in the rightmost digit as determined by the standard error.

τ_c (ns)	R_A	R_B	R_{AB}	$R_{\mathrm{acc}}^{(m)}$	$R_{\mathrm{acc}}^{(2r)}$	α_{2d}
45.51	422 400	425 300	20 200	8200	8180	2.47(2)
18.15	422 500	425 500	15 200	3280	3250	4.68(6)
12.31	422 400	425 900	14 200	2230	2210	6.41(7)
8.12	422 400	425 300	13 400	1480	1460	9.2(1)
45.51	101 700	101 200	3340	465	469	7.13(6)
18.15	101 700	101 200	3040	187	186	16.3(2)
12.31	101 700	101 300	2970	129	127	23.4(3)
8.12	101 800	101 200	2920	85.3	83.7	34.9(5)

We note that Eq. (A7) is still an excellent approximation for accidental coincidences. We also see substantially more singles and coincidence counts compared to our earlier experiment (see Table II). Unfortunately, the accidental coincidences have increased even more, causing the anticorrelation parameter to be significantly lower. Thus, the removal of the bandpass filters degrades the experimental results. In other words, the use of bandpass filters improves the correlation between the two arms of the down-converted light source.

Let us examine this situation a little more closely. Because we suspect that there are significant nontwin events in this experiment, there is no way to solve Eqs. (A2)–(A6) without additional information. However, we can use the results of the same experiment with bandpass filters to provide the necessary data. The only difference between these two experiments is the removal of the bandpass filters, which increases the overall efficiency of the system and possibly the nontwin and background events measured by the detectors. However, it has no effect on $R^{(t)}$ (although it will certainly affect the twins measured by the detectors). Thus, $R^{(t)}$ remains the same when the filters are removed.

Knowing $R^{(t)}$, we can use Eq. (A5) to determine the efficiencies of the system if we assume that the efficiencies of the A and B lines are the same. Based on our previous results, this assumption appears to be reasonable. We have

$$R_{AB}^{(\mathrm{real})} = R_{AB} - \tau_c R_A R_B = \eta^2 R^{(t)}, \tag{A16}$$

from which we obtain $\eta \approx 10.4\%$ for the higher-count-rate data and $\eta \approx 10.6\%$ for the lower-count-rate data. Equations (A2) and (A3) can then be used to determine the rate of non-twins measured by the detectors. We find that approximately 75% of the singles rates are now due to nontwin events. Because these nontwin events lead to accidental coincidences, the removal of the bandpass filters increases the "noise" in the system. Although the efficiencies of the system are reduced with the use of bandpass filters, viewed in this way the signal-to-noise ratio improves.

APPENDIX B: REDUCING α_{3d}

In Sec. III A we discussed a three-detector anticorrelation experiment that would ideally give $\alpha_{3d}=0$. Here we investigate what factors affect α_{3d}. For simplicity, we restrict our attention to a situation in which the only events registered by the detectors are due to down-conversion twins. As before, we let $R^{(t)}$ be the rate of twins heading toward the detector couplers and let η_A, η_B, and $\eta_{B'}$ be the total efficiencies of the A, B, and B' lines, respectively. Then, for a 50-50 beam splitter (see Fig. 3), the count rates detected in A, B, and B' are

$$R_A \approx \eta_A R^{(t)}, \quad R_{\mathrm{B}} \approx \tfrac{1}{2}\eta_B R^{(t)}, \quad \text{and} \quad R_{B'} \approx \tfrac{1}{2}\eta_{B'} R^{(t)}, \tag{B1}$$

while the twofold coincidences are

$$R_{AB} \approx \tfrac{1}{2}\eta_A \eta_B R^{(t)} \quad \text{and} \quad R_{AB'} \approx \tfrac{1}{2}\eta_A \eta_{B'} R^{(t)}. \tag{B2}$$

In Sec. III B we showed that Eq. (9) accounted for all of the measured triple coincidences. If we replace $R_{ABB'}$ in Eq. (8) by the right-hand side of Eq. (9) and use Eqs. (B1) and (B2), we can reduce the anti-correlation parameter to

$$\alpha_{3\mathrm{d}} \approx \left(\frac{R_{B'}}{R_{AB'}} + \frac{R_B}{R_{AB}}\right)\tau_c R_A \approx 2\tau_c R^{(t)}. \tag{B3}$$

In this form we see that α_{3d} is proportional to the coincidence window and the twin count rate; the efficiencies have no effect. While τ_c is determined by the hardware, $R^{(t)}$ is continuously variable by adjusting the input laser power. This variability makes it straightforward to test the predicted relation between α_{3d} and $R^{(t)}$ given in Eq. (B3). As shown in Fig. 6, the linearity is clearly evident in our results (see also Refs. 30 and 40).

Interestingly, the slope of the best-fit line in Fig. 6 is 6.1 ns, somewhat less than our previously measured $\tau_c=8.12$ ns. Although part of the discrepancy might arise from the approximations used in deriving Eq. (B3), we also

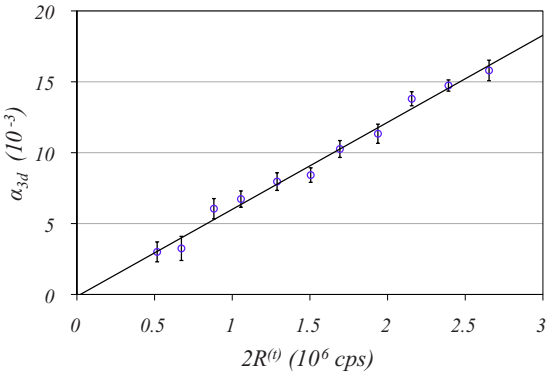

Fig. 6. Three-detector anticorrelation parameter α_{3d} as a function of the twin production rate $2R^{(t)}$. The error bars denote the standard error.

made the implicit assumption that a coincidence between a random single event and a real twin event would have the same coincidence window as a coincidence between two random single events. This assumption should hold if the twin event results in two pulses that leave the single-photon counting module at exactly the same instant. Evidently this assumption is not applicable. Our results suggest that there is a ≈ 2 ns average delay time between the two channels of our single-photon counting module. We are investigating this delay further and will report the results elsewhere.

[a]Electronic mail: pearsonb@dickinson.edu

[1] Rovert Q. Stanley, "Question #45. What (if anything) does the photoelectric effect teach us?," Am. J. Phys. **64**, 839–839 (1996).

[2] P. W. Milonni, "Answer to question #45 ['What (if anything) does the photoelectric effect teach us?,' R. Q. Stanley, Am. J. Phys. 64, 839 (1996)]," Am. J. Phys. **65**, 11–12 (1997).

[3] P. A. M. Dirac, "The quantum theory of the emission and absorption of radiation," Proc. R. Soc. London, Ser. A **114**, 243–265 (1927).

[4] Silvan S. Schweber, *QED and the Men Who Made It: Dyson, Feynman, Schwinger, and Tomonga* (Princeton U. P., Princeton, 1994).

[5] Marian O. Scully and Murray Sargent, "The concept of the photon," Phys. Today **25**(3), 38–47 (1972).

[6] R. Hanbury Brown and R. Q. Twiss, "Correlation between photons in two coherent beams of light," Nature (London) **177**, 27–29 (1956).

[7] R. Q. Twiss, A. G. Little, and R. Hanbury Brown, "Correlation between photons, in coherent beams of light, detected by a coincidence counting technique," Nature (London) **180**, 324–326 (1957).

[8] Roy J. Glauber, "Photon correlations," Phys. Rev. Lett. **10**, 84–86 (1963).

[9] Roy J. Glauber, "The quantum theory of optical coherence," Phys. Rev. **130**, 2529–2539 (1963).

[10] Roy J. Glauber, "Coherent and incoherent states of the radiation field," Phys. Rev. **131**, 2766–2788 (1963).

[11] E. C. G. Sudarshan, "Equivalence of semiclassical and quantum mechanical descriptions of statistical light beams," Phys. Rev. Lett. **10**, 277–279 (1963).

[12] P. L. Kelley and W. H. Kleiner, "Theory of electromagnetic field measurement and photoelectron counting," Phys. Rev. **136**, A316–A334 (1964).

[13] L. Mandel and E. Wolf, "Coherence properties of optical fields," Rev. Mod. Phys. **37**, 231–287 (1965).

[14] F. T. Arecchi, E. Gatti, and A. Sona, "Time distribution of photons from coherent and Gaussian sources," Phys. Lett. **20**, 27–29 (1966).

[15] David C. Burnham and Donald L. Weinberg, "Observation of simultaneity in parametric production of optical photon pairs," Phys. Rev. Lett. **25**, 84–87 (1970).

[16] John F. Clauser, "Experimental limitations to the validity of semiclassical radiation theories," Phys. Rev. A **6**, 49–54 (1972).

[17] John F. Clauser, "Experimental distinction between the quantum and classical field-theoretic predictions for the photoelectric effect," Phys. Rev. D **9**, 853–860 (1974).

[18] H. J. Kimble, M. Dagenais, and L. Mandel, "Photon antibunching in resonance fluorescence," Phys. Rev. Lett. **39**, 691–695 (1977).

[19] P. Grangier, G. Roger, and A. Aspect, "Experimental evidence for a photon anticorrelation effect on a beam splitter: A new light on single-photon interferences," Europhys. Lett. **1**, 173–179 (1986).

[20] Gilbert N. Lewis, "The conservation of photons," Nature (London) **118**, 874–875 (1926).

[21] W. E. Lamb, Jr., "Anti-photon," Opt. Photonics News **60**, 77–84 (1995).

[22] *The nature of light: What is a photon?*, edited by Chandrasekhar Roychoudhuri, A. F. Kracklauer, and Katherine Creath (CRC Press/Taylor & Francis Group, Boca Raton, FL, 2008).

[23] T. J. Axon, "Introducing Schrödinger's cat in the laboratory," Am. J. Phys. **57**, 317–321 (1989).

[24] P. Koczyk, P. Wiewior, and C. Radzewicz, "Photon counting statistics—Undergraduate experiment," Am. J. Phys. **64**, 240–245 (1996).

[25] A. C. Funk and M. Beck, "Sub-Poissonian photocurrent statistics: Theory and undergraduate experiment," Am. J. Phys. **65**, 492–500 (1997).

[26] C. H. Holbrow, E. Galvez, and M. E. Parks, "Photon quantum mechanics and beam splitters," Am. J. Phys. **70**, 260–265 (2002).

[27] E. J. Galvez, C. H. Holbrow, M. J. Pysher, J. W. Martin, N. Courtemanche, L. Heilig, and J. Spencer, "Interference with correlated photons: Five quantum mechanics experiments for undergraduates," Am. J. Phys. **73**, 127–140 (2005).

[28] Dietrich Dehlinger and M. W. Mitchell, "Entangled photon apparatus for the undergraduate laboratory," Am. J. Phys. **70**, 898–902 (2002).

[29] Dietrich Dehlinger and M. W. Mitchell, "Entangled photons, nonlocality, and Bell inequalities in the undergraduate laboratory," Am. J. Phys. **70**, 903–910 (2002).

[30] J. J. Thorn, M. S. Neel, V. W. Donato, G. S. Bergreen, R. E. Davies, and M. Beck, "Observing the quantum behavior of light in an undergraduate laboratory," Am. J. Phys. **72**, 1210–1219 (2004).

[31] A. Gogo, W. D. Snyder, and M. Beck, "Comparing quantum and classical correlations in a quantum eraser," Phys. Rev. A **71**, 052103-1–6 (2005).

[32] We use handheld radiation sensors from Vernier Software and Technology and 2-μCi radium sources, but any low-level source and radiation sensor should work well. By changing the distance between the source and the detector, our count rates vary from a few cps to thousands of cps.

[33] Phillip R. Bevington, *Data Reduction and Error Analysis for the Physical Sciences* (McGraw-Hill, New York, 1969).

[34] In reality, the coincidence window will be slightly smaller because there is some minimum overlap necessary to trigger the electronics. This equation holds if τ represents the effective pulse width.

[35] Carl Eckart and Francis R. Shonka, "Accidental coincidences in counter circuits," Phys. Rev. **53**, 752–756 (1938).

[36] Because highly correlated measurements lead to large values of α, it seems reasonable to refer to α as the correlation parameter. However, to avoid unnecessary confusion, we stick with the current terminology.

[37] In the optics community the anticorrelation parameter corresponds to the degree of second-order temporal coherence at zero time delay, $g^{(2)}(0)$ (Refs. 30 and 38). A fully quantum-optical treatment (which we do not do with our students) produces the same result (Refs. 40 and 48).

[38] Rodney Loudon, *The Quantum Theory of Light*, 3rd ed. (Oxford U. P., Oxford, 2000).

[39] George Greenstein and Arthur G. Zajonc, *The Quantum Challenge: Modern Research on the Foundations of Quantum Mechanics*, 2nd ed. (Jones and Bartlett, Sudbury, MA, 2006).

[40] M. Beck, "Comparing measurements of $g^{(2)}(0)$ performed with different coincidence detection techniques," J. Opt. Soc. Am. B **24**, 2972–2978 (2007).

[41] D. Branning, S. Bhandari, and M. Beck, "Low-cost coincidence-counting electronics for undergraduate quantum optics," Am. J. Phys. **77**, 667–670 (2009).

[42] See: ⟨www.whitman.edu/beckmk/QM/⟩.

[43] Incandescent light is an example of a multimode thermal source. For our purposes the important point is that the statistics of such a source are, to an excellent approximation, Poissonian.

[44] A good set of homework or prelab questions is for students to estimate by what factor the light will need to be dimmed so as not to damage the single-photon counting module. Although the 780 nm long-pass filters provide much of this filtering, we still need to dim the minimaglite by approximately a factor of 1000.

[45] Students can be challenged to determine the necessary filtering. In our case the laser must be dimmed by an additional factor of approximately 10^7.

[46] The fluctuations in the singles counts are dominated by the stability of the laser and are therefore not Poissonian for higher count rates.

[47] M. O. Scully and W. E. Lamb, Jr., "Quantum theory of an optical maser. III. Theory of photoelectron counting statistics," Phys. Rev. **179**, 368–374 (1969).

[48] Leonard Mandel and Emil Wolf, *Optical Coherence and Quantum Optics* (Cambridge U. P., Cambridge, 1995).

[49] Christopher C. Gerry and Peter L. Knight, *Introductory Quantum Optics* (Cambridge U. P., Cambridge, 2005).

[50] Mark B. Schneider and Indhira A. LaPuma, "A simple experiment for discussion of quantum interference and which-way measurement," Am. J. Phys. **70**, 266–271 (2002).

[51] T. L. Dimitrova and A. Weis, "The wave particle duality of light: A demonstration experiment," Am. J. Phys. **76**, 137–142 (2008).

[52] Amnon Yariv, *Quantum Electronics*, 3rd ed. (Wiley, New York, 1989).

[53] C. K. Hong and L. Mandel, "Experimental realization of a one-photon localized state," Phys. Rev. Lett. **56**, 58–60 (1986).

[54] We use the same back-alignment procedure for coupler B' as we use for couplers A and B.

[55] Brahim Lounis and Michel Orrit, "Single-photon sources," Rep. Prog. Phys. **68**, 1129–1179 (2005).
[56] Using a HeNe we carefully align the beams parallel to the holes in the optical table at each stage of the process (using irises). This alignment guarantees the path lengths will be close enough to observe white light fringes using a spectrometer. Tweaking the movable mirror until all wavelengths interfere constructively gives us equal path lengths. Finally, we use a fiber-coupled laser to "back align" the detector couplers through the Mach–Zehnder interferometer to be parallel to one of the down-conversion arms.
[57] The coherence length can be estimated as follows. The frequency of the light f is given by $f=c/\lambda$. For a wavelength of $\lambda=810$ nm and a bandwidth of $\Delta\lambda\approx 10$ nm, the coherence length can be calculated as $L_c\approx c/\Delta f\approx 65\ \mu$m.
[58] Richard P. Feynman, Robert B. Leighton, and Matthew Sands, *The Feynman Lectures on Physics* (Addison-Wesley, Boston, 1963), Vol. 3.
[59] Although not shown in Fig. 5, interference fringes do not return in the B' detector because these photons still carry path information.
[60] J. A. Carlson, M. D. Olmstead, and Mark Beck, "Quantum mysteries tested: An experiment implementing Hardy's test of local realism," Am. J. Phys. **74**, 180–186 (2006).
[61] Thomas A. Moore, *Six Ideas That Shaped Physics, Unit Q: Particles Behave Like Waves*, 2nd ed. (McGraw-Hill, New York, 2003).
[62] Daniel M. Greenberger, Michael A. Horne, and Anton Zeilinger, "Multiparticle interferometry and the superposition principle," Phys. Today **46** (8), 22–29 (1993).
[63] We choose $\theta=-\pi/4$ instead of $\pi/4$ to keep the interference pattern in phase with the original interference pattern.
[64] Richard P. Feynman, "Space-time approach to non-relativistic quantum mechanics," Rev. Mod. Phys. **20**, 367–387 (1948).
[65] P. G. Kwiat, A. M. Steinberg, R. Y. Chiao, P. H. Eberhard, and M. D. Petroff, "Absolute efficiency and time-response measurement of single-photon detectors," Appl. Opt. **33**, 1844–1853 (1994).
[66] For example, Ref. 65 begins with these simple equations before discussing modifications.

Waves in Free Space
Bob Panoff, Shodor Foundation
Tune: Home on the Range

O, E is a field
Whose divergence will yield
The charge density times four pi.
Its curl is B dot,
Hence, in statics it's naught;
And the flux rate is just minus I.

Waves, waves in free space.
At the speed of light c they do hurl.
They flux energy as their modes E and B
Oscillate with divergenceless curl.

No monopoles yet,
So del dot B is nyet,
But the search will go with new toys.
As waves impact matter,
They reflect and back-scatter.
Transforms filter signals from noise.

Waves, waves in free space.
At the speed of light c they do hurl.
They flux energy as their modes E and B
Oscillate with divergenceless curl.

The curl of B is dE by dt
If charges move, add in Jf.
But don't be a fool
Cuz' there's no left-hand rule:
So only the right one is left.

Waves, waves in free space.
At the speed of light c they do hurl.
They flux energy as their modes E and B
Oscillate with divergenceless curl.